

Search for W production using the hadronic decay channel in ep collisions at HERA

ZEUS Collaboration

Abstract

A search for the process $ep \rightarrow eWX$, with the subsequent decay $W \rightarrow qq'$, is performed on 120 pb^{-1} of ep collision data, taken with the ZEUS detector during the 1996-2000 running period. The process leads to final states with two jets of high transverse momentum coming from the W decay and, in some cases, a third jet from the struck quark or, for high values of the negative of the four-momentum-transfer squared Q^2 , a scattered electron with high transverse momentum. The analysis is performed on three different event topologies (two-jets, two-jets and electron, three-jets) and the results are combined to give information on the cross section for $ep \rightarrow eWX$.

1 Introduction

This paper reports the results of an investigation of the production of W bosons in electron¹-proton collisions at center-of-mass energy 300 and 318 GeV at HERA. Single W production is a rare Standard Model (SM) process and an important source of background to searches for physics beyond the Standard Model [1, 2]. Investigations of the process $ep \rightarrow eWX$, $W \rightarrow l\nu$, where $l = \mu, e$ have been performed at HERA by both the H1 [2, 3] and ZEUS [1, 4] collaborations. H1 observes an excess of events with isolated muons or electrons and high missing transverse momentum over the SM prediction, dominated by single W production. The ZEUS results do not confirm this excess. Therefore a complementary study of W production at HERA where the W decays hadronically can yield important information.

The dominant leading order Feynman diagrams for single W production at HERA are shown in Figure 1. In the hadronic decay channel of the W , the event topology contains two or three high transverse energy (E_T^{jet}) jets. If the negative of the four-momentum transfer squared (Q^2) is greater than a few GeV^2 , the scattered electron can be observed in the detector.

The study was performed by selecting events containing at least two high transverse energy jets. The sample was then subdivided according to three mutually exclusive characteristic topologies: (1) events containing 2 high E_T jets, (2) events containing 3 jets and (3) events containing 2 jets and 1 isolated electron. The data set corresponds to the 1996-2000 running period, with a total integrated luminosity of 120 pb^{-1} .

2 Monte Carlo simulation of the signal $ep \rightarrow eWX$ and of the background

The leading order (LO) cross section for $ep \rightarrow eWX$ has been calculated using the EPVEC generator [5]. EPVEC calculates the cross section in two regions, corresponding to photoproduction and deep inelastic scattering, which are separated by a cut on the variable u , defined as $(p_q - p_W)$, where p_q and p_W are the 4-momenta of the initial state quark and of the W , respectively. The photon (proton) structure functions used in the calculation are GRV-G(LO) (CTEQ4D). The final state simulation does not include hard gluon radiation.

Such calculations yield a total cross section of 0.945 pb for $\sqrt{s} = 300$ GeV and 1.09 pb for $\sqrt{s} = 320$ GeV. The uncertainties on this value are approximately 5% for the choice

¹ In this paper “electron” refers both to electrons and positrons unless specified.

of u_{cut} (set at 25 GeV^2), 5% for the choice of proton structure function, 10% for photon structure function and 10% from the choice of Q^2 scale [6] used in EPVEC. Next-to-leading order corrections were calculated in [7] and were found to be of the order of 10%. They were however neglected in this analysis.

The most important background to W production in the hadronic decay channel arises from multi-jet production in direct and resolved photoproduction (PHP) and in deep inelastic scattering (DIS) events. PHP events were simulated using the event generator PYTHIA 6.2 [8]. DIS events, which are a large background to the 2 jets and electron topology, have been simulated using the generator DJANGO6 [9], an interface to the Monte Carlo (MC) programs HERACLES 4.5 [10] and LEPTO 6.5 [11]. Leading order QCD and electroweak radiative corrections were included and higher order QCD effects were simulated via parton cascades using the colour-dipole model ARIADNE [12] or parton shower based on a leading-logarithm approximation (MEPS). The hadronisation of the partonic final state was performed by JETSET [13]. The generated events were passed through the GEANT 3.13-based [14] ZEUS detector and trigger simulation programs [15]. They were reconstructed and analysed by the same program chain as the data.

3 The ZEUS detector

A detailed description of the ZEUS detector can be found elsewhere [15]. The main components used in this analysis were the compensating uranium-scintillator calorimeter and the central tracking detector.

The high-resolution uranium–scintillator calorimeter (CAL) [16] consists of three parts: the forward (FCAL), the barrel (BCAL) and the rear (RCAL) calorimeters. Each part is subdivided transversely into towers and longitudinally into one electromagnetic section (EMC) and either one (in RCAL) or two (in BCAL and FCAL) hadronic sections (HAC). The smallest subdivision of the calorimeter is called a cell. The CAL energy resolutions, as measured under test-beam conditions, are $\sigma(E)/E = 0.18/\sqrt{E}$ for electrons and $\sigma(E)/E = 0.35/\sqrt{E}$ for hadrons (E in GeV).

Charged particles are tracked in the central tracking detector (CTD) [17], which operates in a magnetic field of 1.43 T provided by a thin superconducting coil. The CTD consists of 72 cylindrical drift chamber layers, organized in 9 superlayers covering the

polar-angle² region $15^\circ < \theta < 164^\circ$. The transverse-momentum resolution for full-length tracks is $\sigma(p_T)/p_T = 0.0058p_T \oplus 0.0065 \oplus 0.0014/p_T$, with p_T in GeV.

A three-level trigger was used to select events online [18] requiring large total transverse energy and events with two or more high transverse energy jets. Algorithms based on the tracking rejected non- ep collisions consisting mainly of proton beam-gas interactions.

4 Event Reconstruction and Data Selection

Jets in the final state were reconstructed from the energy deposits in the CAL cells using the inclusive longitudinally invariant k_T cluster algorithm [19, 20]. Variables associated with the jets are: the transverse energy E_T^{jet} , the pseudorapidity η^{jet} and the azimuthal angle ϕ^{jet} . The energy of the jets was corrected for losses in dead material.

The absolute value of the cosine of the decay angle in the centre of mass frame of the two highest E_T jets, $|\cos\theta^*|$, defined as:

$$|\cos\theta^*| = \left| \tanh \frac{1}{2}(\eta^{\text{jet}1} - \eta^{\text{jet}2}) \right|, \quad (1)$$

is used to distinguish the signal from the background. The distribution of $|\cos\theta^*|$ is flat for W production, whereas it peaks towards high values (≈ 1) in direct and resolved photoproduction and in deep inelastic scattering.

Longitudinal momentum conservation ensures that $E - p_z$, defined as:

$$E - p_z = \sum_i E_i(1 - \cos\theta_i), \quad (2)$$

where the E_i are the energies deposited in the calorimeter cells, and θ_i are the polar angles at which the cells lie, peaks at twice the electron beam energy E_e for fully contained events. Small values of $E - p_z$ are expected for proton-gas interactions. Values much greater than $2E_e = 55$ GeV are usually caused by superposition of two processes at the same bunch crossing such as deep inelastic scattering overlapping a beam gas event.

Events that pass the trigger requirements were further required to have at least 2 jets with $E_T^{\text{jet}} > 20$ GeV lying in the η^{jet} range $-1.0 < \eta^{\text{jet}} < 2.75$. Other preselection cuts

² The ZEUS coordinate system is a right-handed Cartesian system, with the Z axis pointing in the proton beam direction, referred to as the “forward direction”, and the X axis pointing left towards the center of HERA. The coordinate origin is at the nominal interaction point. The pseudorapidity is defined as $\eta = -\ln(\tan \frac{\theta}{2})$, where the polar angle, θ , is measured with respect to the proton beam direction.

required that the Z -coordinate of the tracking vertex be reconstructed within 50 cm of the nominal interaction point and that $10 \text{ GeV} < E - p_z < 65 \text{ GeV}$.

Events surviving the preselection cuts were subdivided into 3 samples: 2 jet (DIJET), 3 jet (TRIJET) and electron (ELEC). Any event that did not fit into these categories was discarded. The criteria used to categorise the events were:

- Events containing two jets with $E_T^{\text{jet}} > 20 \text{ GeV}$ and η^{jet} in the range $-1.0 < \eta^{\text{jet}} < 2.75$ were classified as DIJET events. In addition it was required that there be no electron candidate as defined later.
- The TRIJET topology contained events with three jets as defined above and any number of electrons.
- Events were classified as ELEC if they contained two jets with $E_T^{\text{jet}} > 20 \text{ GeV}$, η^{jet} lying in the range $-1.0 < \eta^{\text{jet}} < 2.75$ and a scattered electron identified using a neural network algorithm [21]. The electron was required to be isolated and have a matching track if its azimuthal angle was within the CTD acceptance. The global $E - P_z$ of the event was required to be greater than 40 GeV.

The number of events in each category is shown in table 1, for the selected data, for the background MC samples (PHP and DIS) and for the signal MC (EPVEC). The number of events for the MC samples are shown normalized to the data luminosity. The discrepancy of approximately 10% in the background MC normalization can be attributed to high-order QCD corrections to the jet cross-sections [1].

5 Results

A comparison of the selected data with the MC background and signal is shown in figure 2, where the light shaded area shows the background MC (PHP+DIS) normalised to luminosity and then multiplied by the appropriate normalisation factor α from table 2, and the dark shaded histogram shows the signal W MC (EPVEC), normalized to the data luminosity. The first row of figure (2) shows (a) the transverse energy of the two jets, (b) the pseudorapidity of the 2 jets and (c) the $|\cos\theta^*|$ for the DIJET sample. The second row shows (d) the transverse energy of the third highest E_T jet, (e) the pseudorapidity of the third jet and (f) the $|\cos\theta^*|$ for the TRIJET sample. The third row shows (g) the transverse energy of the two jets, (h) the pseudorapidity of the 2 jets and (i) y_e of the electron³.

³ $y_e = 1 - \frac{E_{\text{elec}}}{2E_e}(1 - \cos\theta_e)$ where E_{elec} is the energy of the electron, E_e is the energy of the electron beam, and θ_e is the polar angle of the electron.

The data and background MC show very good agreement in the shape of the distributions. In all topologies the background is very large compared to the signal. Therefore, in order to enhance the signal, a further cut on $|\cos\theta^*|$ was applied to all three samples (< 0.6 to DIJET, 0.7 to TRIJET and 0.65 to ELEC). In addition, in the ELEC sample, a cut of $y_e > 0.2$ was applied. Cuts on these variables were obtained by performing an optimisation routine to maximise the ratio of the number of signal events to the square root of the number of background events in the signal mass window.

Figure 3 shows the invariant mass spectrum of the two highest E_T^{jet} jets (M_{jj}) for the 3 samples (a) DIJET, (b) TRIJET and (c) ELEC, after applying these two additional cuts. From MC studies of the TRIJET events, the two jets coming from the hadronic W-decay are the two highest E_T^{jets} jets in 80% of the cases. The reconstructed invariant mass for the signal is shown as the dark-shaded area in fig. 3. Even after applying the cut on $|\cos\theta^*|$ the background dominates the cross-section.

In order to estimate the cross section for $e \rightarrow eWX$ a binned χ^2 fit of the invariant mass spectrum for signal and background Monte Carlo to data was performed, in a mass window $60 < M_{jj} < 130 \text{ GeV}$:

$$N^{\text{data}} = \alpha N^{\text{bkg}} + \beta N^{\text{Wmc}}, \quad (3)$$

where N^{data} is the number of data events in each bin, N^{bkg} is the number of background events and N^{Wmc} is the number of signal MC events.

The two normalization factors α and β obtained from the fit for the 3 different samples are shown in table 2. The resulting W cross-section estimates, which are obtained multiplying the factors β by the cross-section predicted by the W MC, are shown in the last line of table 2. For the fit only the statistical errors are taken into account. The systematic errors on α and β were estimated by:

- using the MEPS model, instead of the Ariadne model, for the DIS contribution to the background.
- fixing the normalisation of the DIS contribution to the background using the MC cross-section and data luminosity.
- fixing the normalisation of the PHP contribution to the background using the number of data events in the $40 < M_{jj}(\text{GeV}) < 60$ mass window.
- varying the absolute energy scale of the CAL by $\pm 1\%$.

These systematic uncertainties were added in quadrature and the combined errors are shown table 2.

By combining the results from the three channels, a cross-section of:

$$\sigma(ep \rightarrow eWX) = 2.97 \pm 2.51(\text{stat.})_{-0.53}^{+1.75}(\text{syst.}) \text{ pb} \quad (4)$$

was obtained.

In order to set a 95% confidence limit on the cross section for W production, a Bayesian approach with a prior flat in the cross section for $\sigma \geq 0$ and vanishing for $\sigma < 0$ was used, the limit thus obtained was:

$$\sigma(ep \rightarrow eWX) < 8.3 \text{ pb.} \quad (5)$$

6 Summary

A search was made for the hadronic decay of singly produced W bosons at HERA in electron-proton collisions at centre-of-mass energies of 300 and 318 GeV using an integrated luminosity of 120 pb^{-1} . The selected samples with 2 jets, 3 jets, or 2 jets and a scattered electron are dominated by the background due to QCD multi-jet production in photoproduction and deep inelastic scattering events. A fit to the invariant mass of the two highest transverse energy jets was used to extract a W production cross section of $2.97 \pm 2.51(\text{stat.})_{-0.53}^{+1.75}(\text{syst.}) \text{ pb}$. Although the W hadronic-decay channel is not competitive with the leptonic-decay channel and the errors are large, the result shows no anomaly compared to the Standard Model prediction.

References

- [1] ZEUS Coll., S. Chekanov et al., Preprint DESY-03-012 (hep-ex/0302010), DESY, 2003. Acc. by Phys. Lett. B.
- [2] H1 Coll., Preprint DESY-02-022 (hep-ex/0301030), DESY, 2002.
- [3] H1 Coll., C. Adloff et al., Eur. Phys. J. C **5**, 575 (1998).
- [4] ZEUS Coll., J. Breitweg et al., Phys. Lett. B **471**, 411 (2000).
- [5] U. Baur, J.A.M. Vermaseren and D. Zeppenfeld, Nucl. Phys. B **375**, 3 (1992).
- [6] D. Waters, 'A First Estimate of $\sigma(e^+p \rightarrow e^+W^\pm X)$ And Studies Of High P_T Leptons Using The ZEUS Detector. Ph.D. Thesis, University of Oxford, 1998.
- [7] Diener, Schwanenberger and Spira, Preprint DESY-02-035 (hep-ph/0203269), 2002.
- [8] T. Sjöstrand, L Lönnblad, Comp. Phys. Comm. **135**, 238 (2001).
- [9] K. Charchula, G.A. Schuler and H. Spiesberger, Comp. Phys. Comm. **81**, 381 (1994).
- [10] A. Kwiatkowski, H. Spiesberger and H.-J. Möhring, Comp. Phys. Comm. **69**, 155 (1992). Also in *Proc. Workshop Physics at HERA*, 1991, DESY, Hamburg.
- [11] G. Ingelman, A. Edin and J. Rathsman, Comp. Phys. Comm. **101**, 108 (1997).
- [12] L. Lönnblad, Comp. Phys. Comm. **71**, 15 (1992).
- [13] T. Sjöstrand, Comp. Phys. Comm. **39**, 347 (1986).
- [14] R. Brun et al., GEANT3, Technical Report CERN-DD/EE/84-1, CERN, 1987.
- [15] ZEUS Coll., U. Holm (ed.), *The ZEUS Detector*. Status Report (unpublished), DESY (1993), available on <http://www-zeus.desy.de/bluebook/bluebook.html>.
- [16] M. Derrick et al., Nucl. Inst. Meth. A **309**, 77 (1991);
A. Andresen et al., Nucl. Inst. Meth. A **309**, 101 (1991);
A. Caldwell et al., Nucl. Inst. Meth. A **321**, 356 (1992);
A. Bernstein et al., Nucl. Inst. Meth. A **336**, 23 (1993).
- [17] N. Harnew et al., Nucl. Inst. Meth. A **279**, 290 (1989);
B. Foster et al., Nucl. Phys. Proc. Suppl. B **32**, 181 (1993);
B. Foster et al., Nucl. Inst. Meth. A **338**, 254 (1994).
- [18] ZEUS Coll., M. Derrick et al., Phys. Lett. B **293**, 465 (1992).
- [19] S. Catani et al., Nucl. Phys. B **406**, 187 (1993).
- [20] S.D. Ellis and D.E. Soper, Phys. Rev. D **48**, 3160 (1993).
- [21] H. Abramowicz, A. Caldwell and R. Sinkus, Nucl. Inst. Meth. A **365**, 508 (1995).

	DIJET	TRIJET	ELEC
Data	19338	3002	4986
Signal	27.39	12.43	5.42
Background	17398	2286	4747

Table 1: Events in each event class after preselection cuts.

	DIJET	TRIJET	ELEC	Combined
β	$3.39^{+3.14}_{-3.14}$	$2.04^{+3.59}_{-3.64}$	$1.35^{+9.47}_{-9.54}$	—
α	$1.12^{+0.01}_{-0.01}$	$1.32^{+0.05}_{-0.05}$	$1.01^{+0.03}_{-0.03}$	—
χ^2/ndef	7.86/12	18.33/12	13.38/12	—
σ/pb	$3.69^{+3.42}_{-3.42}$	$2.23^{+3.91}_{-3.97}$	$1.47^{+10.31}_{-10.39}$	$2.97 \pm 2.51(\text{stat.})^{+1.75}_{-0.53}(\text{syst.})$

Table 2: Values of α and β obtained from the fits described in the text. Also shown are the χ^2 value of the fit and the corresponding cross section estimate σ for Single W Production.

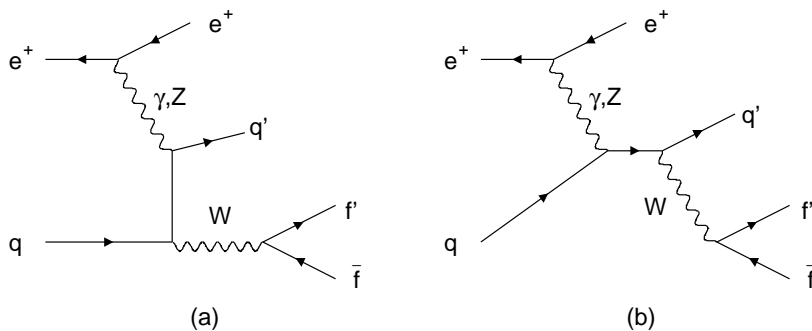


Figure 1: Main leading order Feynman diagrams for the process $ep \rightarrow eWX$.

ZEUS

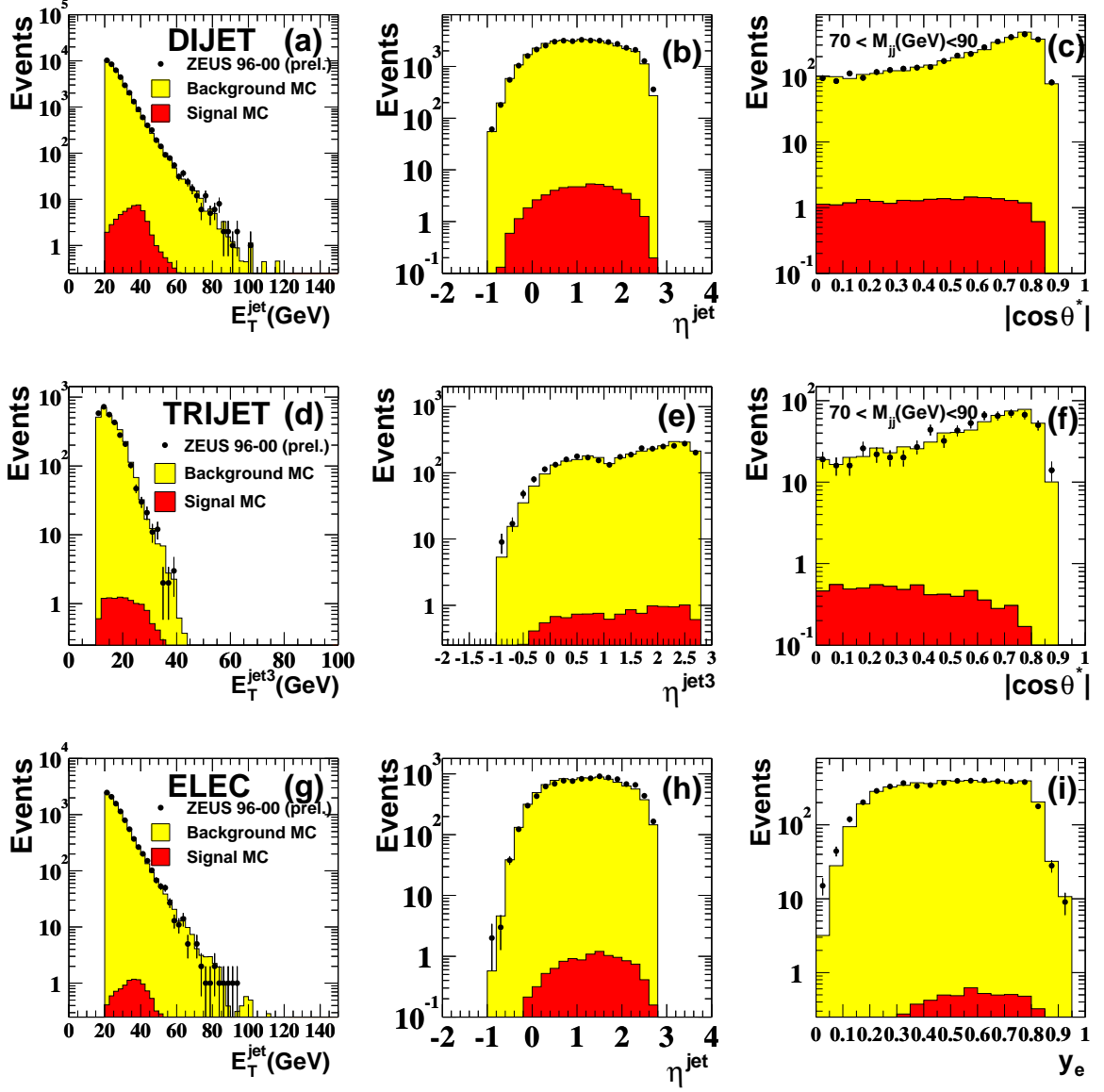


Figure 2: Data (points) compared to combined data-normalised Monte Carlo for the 3 samples. The top row shows variables from the DIJET sample, the middle row from the TRIJET sample and the distributions in the bottom row are from the ELEC sample. The light shaded histogram represents the background (PHP+DIS) MC prediction, the dark shaded area the signal ($W \rightarrow \text{jets}$) prediction. The variables shown are described in detail in the text.

ZEUS

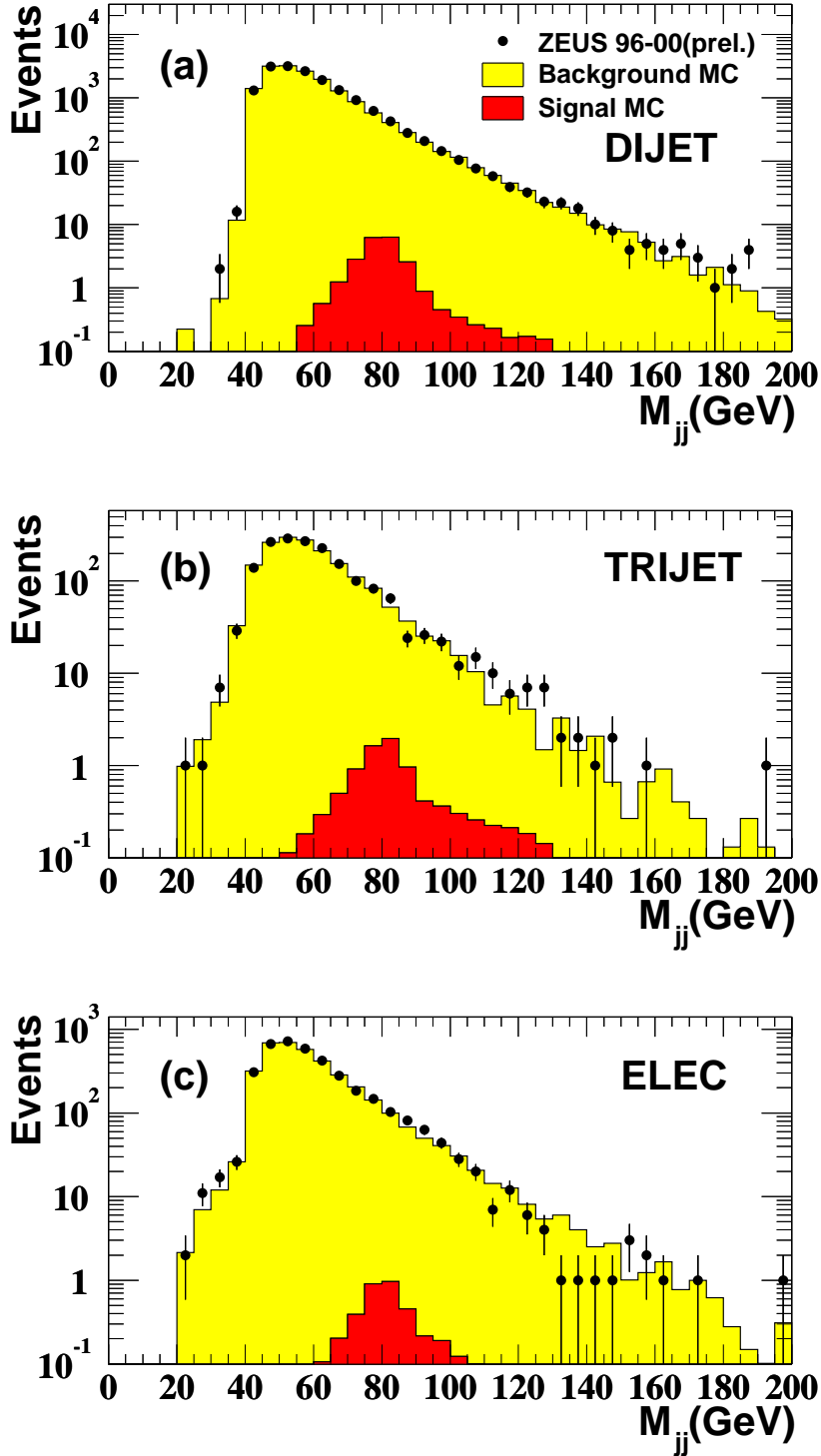


Figure 3: *Invariant mass spectra for (a)DIJET, (b)TRIJET and (c)ELEC samples. The background MC is shown as the light-shaded histogram, normalised with the coefficient α obtained from the fit and shown in table 2. The signal MC is shown as the dark-shaded histogram and is normalised to the data-luminosity.*